



HAL
open science

Ergodic billiard and statistical energy analysis

H. Li, N. Totaro, Laurent Maxit, A. Le Bot

► **To cite this version:**

H. Li, N. Totaro, Laurent Maxit, A. Le Bot. Ergodic billiard and statistical energy analysis. Wave Motion, 2018, 10.1016/j.wavemoti.2018.08.011 . hal-01896738

HAL Id: hal-01896738

<https://hal.science/hal-01896738>

Submitted on 22 Oct 2021

HAL is a multi-disciplinary open access archive for the deposit and dissemination of scientific research documents, whether they are published or not. The documents may come from teaching and research institutions in France or abroad, or from public or private research centers.

L'archive ouverte pluridisciplinaire **HAL**, est destinée au dépôt et à la diffusion de documents scientifiques de niveau recherche, publiés ou non, émanant des établissements d'enseignement et de recherche français ou étrangers, des laboratoires publics ou privés.



Distributed under a Creative Commons Attribution - NonCommercial 4.0 International License

Ergodic billiard and statistical energy analysis

H. Li^{a,b}, N. Totaro^b, L. Maxit^b, A. Le Bot^a

^a*Université de Lyon, École centrale de Lyon, Laboratoire de tribologie et dynamique des systèmes, UMR CNRS 5513, 36, av. Guy de Collongue 69134 Ecully, France*

^b*Université de Lyon, INSA-Lyon, Laboratoire vibrations acoustique, 20 avenue Albert Einstein F-69621 Villeurbanne, France*

Abstract

This paper highlights the importance of ergodicity of billiards in Statistical energy analysis (SEA), a statistical theory of sound and vibration. We show that the main relationship of statistical energy analysis, the so-called coupling power proportionality, is intimately linked with the establishment of a diffuse vibration field in subsystems. In particular, we show that when subsystems have ergodic geometries or when the nature of excitation enforces a diffuse field, the energy exchange between two weakly coupled subsystems is proportional to the difference of vibrational energies. But when the field is not diffuse (either non isotropic or non homogeneous), the exchange of energy does not generally follow this proportionality. Numerical simulations are provided to support the discussion.

Keywords: Sound and vibration, Structural dynamics, High-frequency, Statistical energy analysis, Ergodic billiard, Diffuse field

1. Introduction

Statistical energy analysis [1] (SEA) is an attractive theory of sound and vibration elaborated in the early sixties [2, 3, 4, 5, 6]. Two reasons at least may explain its popularity.

First, the theory is efficient at high frequencies where no other numerical tool is available. In many industries, such as transportation, building, aerospace, prediction of sound and vibration levels is important to ensure

Email address: alain.le-bot@ec-lyon.fr (A. Le Bot)

Preprint submitted to Wave motion

July 17, 2018

comfort to passengers or integrity of equipment, especially in the audio frequency range. Most often, classical methods such as finite elements reach their limit imposed by the capabilities of computers. Statistical energy analysis then takes over beyond this frequency limit.

Second, the concept of statistical energy analysis leads to a new scientific method applied to sound and vibration. Instead of the classical approach of mechanics in terms of strain and stress, statistical energy analysis proposes an energetic description of systems. It becomes then easier to analyze the systems as energy flowing from source to receiver with the possibility to determine the transfer paths [7, 8, 9]. The second novelty is to introduce a statistical description in vibroacoustics in the same spirit as Sabine's theory of reverberation [10] in acoustics. The gain is simplicity in the theory. But we must give up the idea of a complete and deterministic description of systems. Information on details is lost. And this may even be quantized by introducing vibrational entropy [11, 12, 13]. This is a true change of paradigm [14].

The exact list of assumptions required in statistical energy analysis may vary from one author to the next [15, 16, 17, 18, 19] but the main ones are random forces, weak coupling and high reverberation in all subsystems. Statistical energy analysis is a thermodynamical approach of sound and vibration where the exchange of energy between subsystems is driven by the notion of vibrational temperature. The requirement of reverberation and its consequence - the diffuse field - means that subsystems must be in local thermal equilibrium. Two adjacent subsystems weakly coupled may have different vibrational temperatures leading to exchange energy from 'hot' to 'cold' subsystems.

Reverberation, ergodicity and wave chaos are the key concepts in room acoustics [20, 21] as well as in statistical energy analysis [22]. The link between statistical energy analysis and ray-tracing is particularly apparent in dynamical energy analysis [23] or radiative transfer approach [24]. From complexity in ray propagation emerges simplicity in macroscopic behaviour. The geometrical conditions giving rise to disorder and chaos is a matter for billiard's theory.

The purpose of this paper is to highlight the link between statistical energy analysis and ray dynamics in billiards and more specifically ergodicity. The outline of the paper is as follows. Section 2 presents a short review of statistical energy analysis with a special focus on its assumptions and main result, the coupling power proportionality. The conditions which lead to the emergence of diffuse field is investigated in Section 3. In Section 4, the

validity of the coupling power proportionality is analysed. The paper finishes by some concluding remarks.

2. Statistical energy analysis

The principle of statistical energy analysis is to subdivide a complex system into subsystems and to analyse their exchanges of vibrational energies. Generally, the subsystems correspond to structural elements such as plates, beams, mechanical resonators and acoustical cavities but, more theoretically, they correspond to groups of modes in thermal equilibrium. The vibrational sources are random and have flat spectrum in the frequency band $\Delta\omega$ centred on ω .

Statistical energy analysis requires several assumptions [1, 18]. These are

- (H1) Couplings between subsystems are conservative and weak
- (H2) External sources are random, stationary, uncorrelated, and wideband
- (H3) The field is diffuse in each subsystem

The diffuse field assumption (H3) is certainly the least understood assumption and the most difficult to satisfy in practice. It is commonly admitted that the diffuse field state of vibration naturally emerges in highly reverberant structures, that is with a low damping and with a large number of modes in the frequency band $\Delta\omega$. This is why (H3) is sometimes replaced by the two following assumptions.

- (H4) All subsystems contain a large number of resonant modes
- (H5) All subsystems are lightly damped

As we shall see in this paper, (H4) and (H5) do not necessarily imply (H3). We shall therefore consider systems verifying (H4) and (H5) and explore the conditions for which a diffuse field state is established.

For the sake of simplicity, we limit the discussion in what follows to systems made up with plates in bending vibration and coupled by mechanical springs.

The modal density of plate i defined as the number of modes per unit circular frequency ω (rad/s) is

$$n_i = \frac{A_i}{4\pi} \sqrt{\frac{m_i}{D_i}} \tag{1}$$

where m_i is the mass per unit area, D_i the bending stiffness, and A_i the plate area. The number of resonant modes $N_i = n_i \Delta\omega$ must be large by (H4).

We denote by E_i the expectation of vibrational energy in subsystem i . Expectation must be understood in the meaning of probability theory. This is the mean value for several realizations of the random process associated to excitation forces. By virtue of stationarity (H2), E_i does not depend on time. We also denote by P_{ij} the expectation of vibrational power exchanged between subsystems i and j . Then, the main result of statistical energy analysis states the power being exchanged between subsystems i and j is proportional to the difference of modal energies

$$P_{ij} = \beta_{ij} \left(\frac{E_i}{n_i} - \frac{E_j}{n_j} \right) \quad (2)$$

This is the coupling power proportionality. The conductivity factor β_{ij} verifies reciprocity $\beta_{ij} = \beta_{ji}$. For two plates coupled by a spring, its value is given by [17]

$$\beta_{ij} = \frac{K^2}{32\pi\omega^2 \sqrt{m_i D_i m_j D_j}} \quad (3)$$

where K is the stiffness of the coupling spring.

Assumptions (H1) to (H5) are important requirements to guarantee the validity of the coupling power proportionality. To satisfy (H2), we shall introduce random forces whose spectrum S is constant in an octave band $\Delta\omega$. For the other assumptions, we may introduce several dimensionless factors to check them a priori. The first one is the number of resonant modes $N_i = n_i \Delta\omega$ which must be large to satisfy (H4). Equivalently, the wavelength $\lambda = 2\pi(D_i/m_i)^{1/4}\omega^{-1/2}$ must be short compared to the mean-free-path $\bar{l} = \pi A_i/L_i$, A_i being the plate area and L_i the perimeter. We therefore introduce the number of wavelengths per mean-free-path \bar{l}/λ . For (H5) we must calculate the normalized attenuation factor [25] $\bar{m}_i = \eta_i \omega \bar{l}/c_{g_i}$ where $c_{g_i} = 2(D_i/m_i)^{1/4}\omega^{1/2}$ is the group speed and η_i the damping loss factor. A small value of \bar{m}_i ensures that rays will be reflected a large number of times before to be dissipated. A large modal overlap $M_i = \eta_i \omega n_i$ is also of interest to check that no particular mode can dominate the dynamics. The three dimensionless numbers, number of resonant modes, normalized attenuation factor and modal overlap are sufficient to delimitate the diffuse field zone in the ω, η -plane [26]. Concerning (H1), different parameters were proposed in the literature to characterise the strength of coupling. The first

criterion is the coupling strength [27, 28, 29] $\gamma = 2\beta_{ij}/(\pi M_i M_j)$. We may also introduce the connection strength [17] $\kappa = K/(m_i A_i m_j A_j \omega^4)^{1/2}$ as the quotient of coupling stiffness K divided by plate stiffness $m_i A_i \omega^2$ in $\Delta\omega$ (in fact $\kappa\omega$ is called strength of connection in [17] but we have divided it by ω to get a dimensionless number). A further factor is Smith's criterion [30] $\sigma = \beta_{ij}(1/M_i + 1/M_j)$ defined as the ratio of coupling loss factor to damping loss factor. A low value of σ ensures that loss of energy by coupling is less than internal dissipation. Let us also mention a last definition of weak coupling based on the ratio of decay time of dynamical correlation to escape time of rays [31]. When these dimensionless parameters γ , κ , σ are much lower than one, the weak coupling assumption is respected.

Since the objective of this article is only to investigate the geometrical properties of subsystems, the rest of the discussion will be held under the condition that (H1), (H2), (H4), and (H5) apply and that all above criteria are satisfied.

3. Diffuse field

As we have underlined, the emergence of diffuse field is an imperative condition in statistical energy analysis. A diffuse field is a special state of vibration for which the vibrational energy is homogeneously distributed and the energy propagation is isotropic [32]. These notions of homogeneity and isotropy of vibration may be clarified in the context the mathematical theory of billiards.

3.1. Ray dynamics

Billiards are dynamical systems of particles moving inside walls. A billiard is defined by a bounded two-dimensional domain where a particle moves along straight lines with a constant energy and is subjected to specular reflection each time it impinges on the boundary [33].

The link between mathematical billiards and vibration in structures appears in the context of geometrical acoustics. In the limit of high frequency, waves propagate as rays moving at sound speed and subjected to reflection, refraction, diffraction, absorption. If one restricts to the phenomena of propagation and reflection solely, rays of geometrical acoustics follow the same laws of motion as particles in billiards, the particle path defining the ray.

Ergodicity is an important statistical property of billiards. An ergodic billiard is defined as a billiard for which almost all rays pass through the

vicinity of any point in any direction in the limit of arbitrary large time. The phase-space of a particle moving at constant speed being defined as the space of position and direction of velocity, this means that almost all rays explore all points of phase-space. Of course, this is exactly what is required to obtain a diffuse field. Since a single ray induces a homogeneous and isotropic repartition of energy, a fortiori several rays will do the same. Consequently, a strongly directional point source (all rays start from same point and take same direction) but also point source with uniform directivity (all rays start from same point but in any direction) and rain-on-the-roof sources (all rays start from any point and take any direction) will indifferently lead to a diffuse field in an ergodic billiard.

An example of ergodic billiard is the so-called Bunimovich stadium [34]. Fig. 1a top shows the propagation of a single ray in a stadium. Beyond the overall appearance which presents a certain disorder, it is clear that the ray explores all regions in the stadium. A larger number of reflections would show that the stadium is uniformly colored by the ray path indicating an uniform probability density function of presence in the stadium. Fig. 1b top shows the resulting Poincaré's section. Each dot gives the position of a reflection in the space position defined by the curvilinear abscissa along the boundary and angular momentum defined as the sine of incidence angle with the normal to boundary. The probability density function of presence is uniform in the phase space.

An example of non ergodic billiard is the circular domain [34]. The circle presents the geometrical property that the angular momentum is conserved during propagation. This means that each ray will impinge on the boundary with a constant incidence angle. The ray turns in the circle and may form a closed path, in which case the orbit is periodic, or an open path, in which case the orbit forms a caustic which delimits a shadow zone where the ray never enters. In Poincaré's section shown in Fig. 1b middle, it is apparent that all positions are explored but all with the same value of angular momentum.

The case of a rectangular billiard is intermediate. The examination of ray paths immediately shows that on each edge, the incidence can take only two values of opposite signs. Therefore the angular momentum can take four values as can be observed from Fig. 1b bottom. Concerning the position space, almost all rays entirely explore the domain and the probability density function of presence is uniform in the position space but not in the angular momentum space.

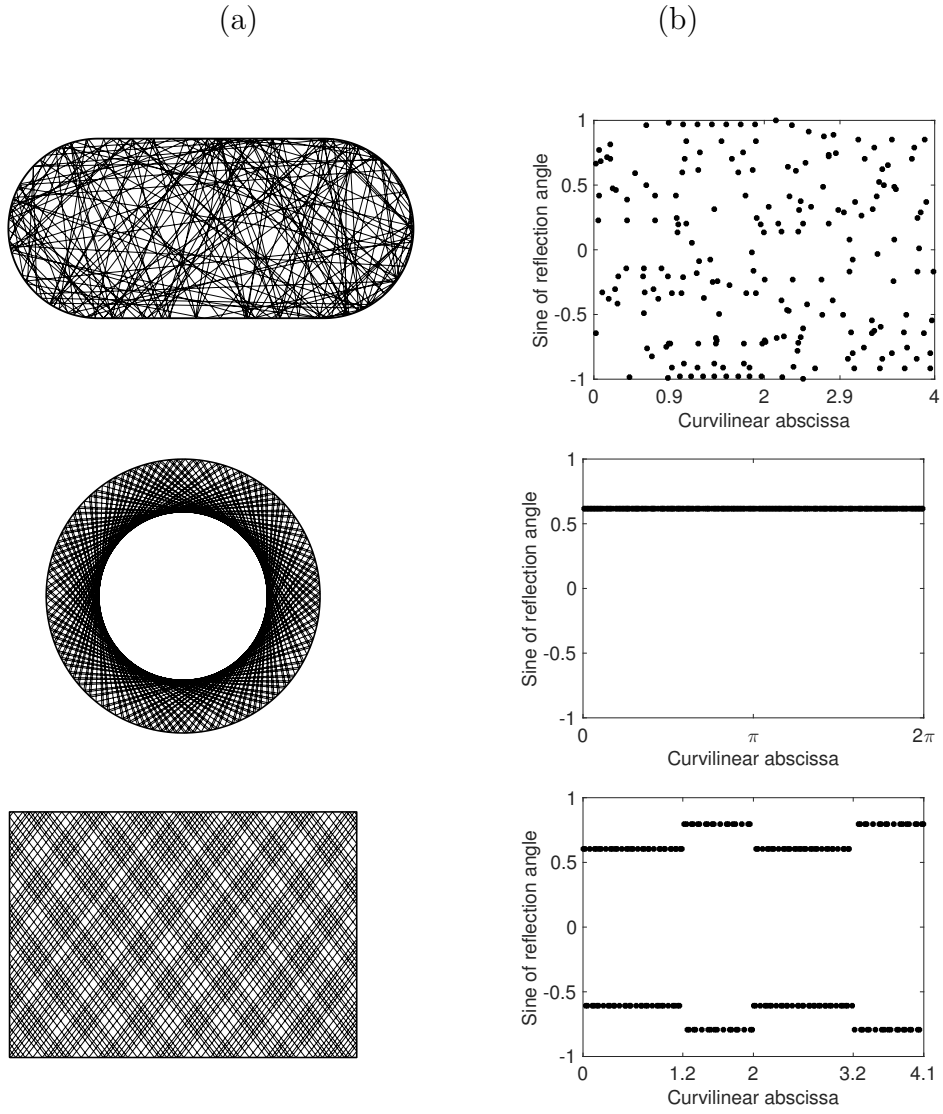


Figure 1: Ray propagation in three billiards: top line, stadium; middle line, circle; bottom line, rectangle. (a), Ray path with 200 reflections; (b), Poincaré's section.

3.2. Vibrational field

We now examine the nature of vibrational field in the plates shown in Fig. 2 excited in bending vibration by a time-varying normal force.

The force field has expression $f(x, y, t) = F(t)\delta(x-x_0)\delta(y-y_0)$ where $F(t)$ is a random force with a power spectral density S constant in the frequency band $[\omega_{\min}, \omega_{\max}]$, δ denotes the Dirac function and the source position is x_0, y_0 . The transverse deflection at time t and position x, y is noted $u(x, y, t)$.

The mean vibrational energy density is taken as twice the mean kinetic energy density

$$W(x, y) = m\langle \dot{u}^2(x, y, t) \rangle \quad (4)$$

where m is the mass per unit area, \dot{u} the vibrational speed of plate and the probability expectation is noted with brackets. In principle, the elastic energy should appear in the above expression but mean kinetic and elastic energy densities are equal when averaged over a small area of the size of a wavelength (except near the boundaries and singularities such as point source or attachment point). Since the random force is stationary, the time no longer appears as variable of W . The total vibrational energy is

$$E = \iint W(x, y) dx dy \quad (5)$$

where the integral is performed over the whole plate surface.

The mean energy density may be calculated by means of the receptance $H(x, y, x_0, y_0; \omega)$ where x, y is the receiver position and x_0, y_0 the source position with harmonic excitation of circular frequency ω . Since the power spectral density S is constant in the band $[\omega_{\min}, \omega_{\max}]$ and zero elsewhere, the mean vibrational energy density is

$$W(x, y) = \frac{S}{\pi} \int_{\omega_{\min}}^{\omega_{\max}} m\omega^2 |H(x, y, x_0, y_0; \omega)|^2 d\omega \quad (6)$$

Note that W also depends on the source position x_0, y_0 . The integral may be approximated using the rectangle rule. The angular frequency step is chosen as $\delta\omega = \omega_{\min}\eta/4$ where η is the damping loss factor. The calculation of energy field in a plate therefore reduces to the calculation of the receptance in the frequency band. More details to calculate the receptance $H(x, y, x_0, y_0; \omega)$ from modes are presented in Appendix.

In what follows, we observe energy fields with a point force excitation in the three plates shown in Fig. 2. The first one is a stadium plate with clamped

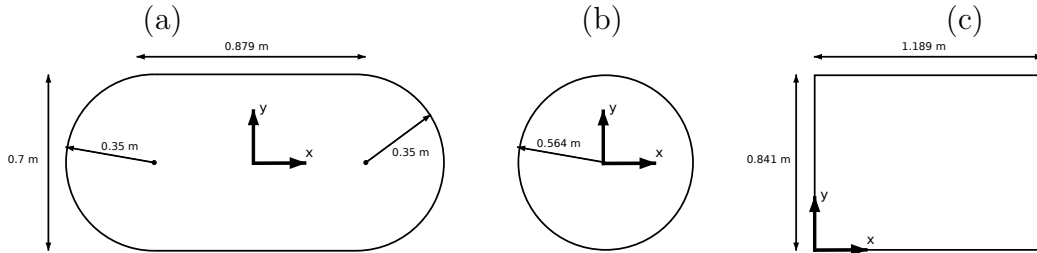


Figure 2: Geometry of plates in numerical examples. (a), stadium; (b), circle; (c), rectangle.

edges, the second one is a circular plate clamped at its edges, and the third one is a rectangular plate with simply supported edges. The geometrical dimensions are chosen such that the surfaces are unity. In addition, the length and width of the rectangular plate are chosen such that their ratio is irrational in order to avoid regularity in the sequence of natural frequencies. The excitation point is located at $x = 0.1643$ m, $y = 0.1767$ m in the stadium plate, at $x = 0.1419$ m, $y = 0.1592$ m in the circular plate and at $x = 0.9689$ m, $y = 0.7617$ m in the rectangular plate (the origin and the reference frame are shown in Fig. 2). The natural frequencies ω_i and mode shapes ψ_i required for the calculation of receptances are obtained in two ways, an analytical method and a finite element method. For rectangular and circular plates, analytical expressions were used for calculation. An additional calculation with the finite element software Nastran was carried out to check the modes and mean vibrational energies under a random excitation. For the stadium plate, modes were computed with Nastran and used for the calculation of receptance as presented in Appendix.

The parameters of the simulations are the following. The plates are all made of steel with Young's modulus $E_0 = 210$ GPa, density $\rho = 7800$ kg m⁻³ and Poisson's ratio $\nu = 0.3$. The plate thickness is 2 mm and the damping loss factor is $\eta = 0.001$. The frequency band of excitation is an octave centred on $\omega_c = 2\pi \times 4000$ rad s⁻¹. The receptances are computed by taking into account all modes from 0 Hz to 11.3 kHz. In each simulation, 30000 receivers are chosen at random on plate to draw the energy density map. In Table 1 are summarized values of number of wavelengths \bar{l}/λ (ratio of mean-free-path to wavelength), the number of resonant modes N , the normalized attenuation \bar{m} and the modal overlap M .

Fig. 3 shows maps of energy level (dB, ref=mean value) and probability

Plate	# Wavelength	# Modes	Attenuation	Modal overlap
Stadium	11.3	450	0.036	0.64
Circle	12.6	450	0.040	0.64
Rectangle	11.0	443	0.035	0.64

Table 1: Number of wavelength \bar{l}/λ , number of resonant modes N , attenuation per mean free path \bar{m} and modal overlap M of plate at 4 kHz

density distribution of energy level in the three plates at the octave 4 kHz.

It may be observed that diffuse vibrations appear on the stadium and the rectangular plate but not on the circular plate. More specifically the energy distributions in rectangular and stadium plates are close to a highly peaked normal distribution while this is not the case for circular plate which presents a wider distribution.

For the stadium plate, homogeneity and isotropy of vibration result from the ergodic characteristic of the corresponding billiard. At 4 kHz the wavelength is $\lambda = 70$ mm which is sufficiently small compared to the mean-free-path $\bar{l} = 0.79$ m to consider that ray approximation is valid. Diffusiveness of vibration in a stadium plate is therefore a consequence of the uniform probability distribution of presence in the phase-space even for a single ray. A point source may be considered as sending rays in all directions. Since each of them induces a diffuse field, the total field induced by all of them is also diffuse.

For the circular plate, the ray dynamics is different since no ray can give rise a diffuse field. More specifically, neither homogeneity nor isotropy can result from ray propagation as it has been seen for a circular billiard. Even though isotropy can originate from the uniform directivity of the point source, the vibrational field never reaches homogeneity. This explains why diffusiveness of vibration is not observed in a circular plate.

For the rectangular plate, homogeneity of vibrational field results from the ray dynamics but not isotropy. However, a point force sends rays in all directions with a uniform directivity under the geometrical acoustics approximation. Since ray direction has a uniform probability density, isotropy is enforced into the vibrational field. In this situation, the vibrational field possesses both homogeneity and isotropy, which creates diffusiveness in a rectangular plate.

It should be noticed that in all these plates there exists a peak of en-

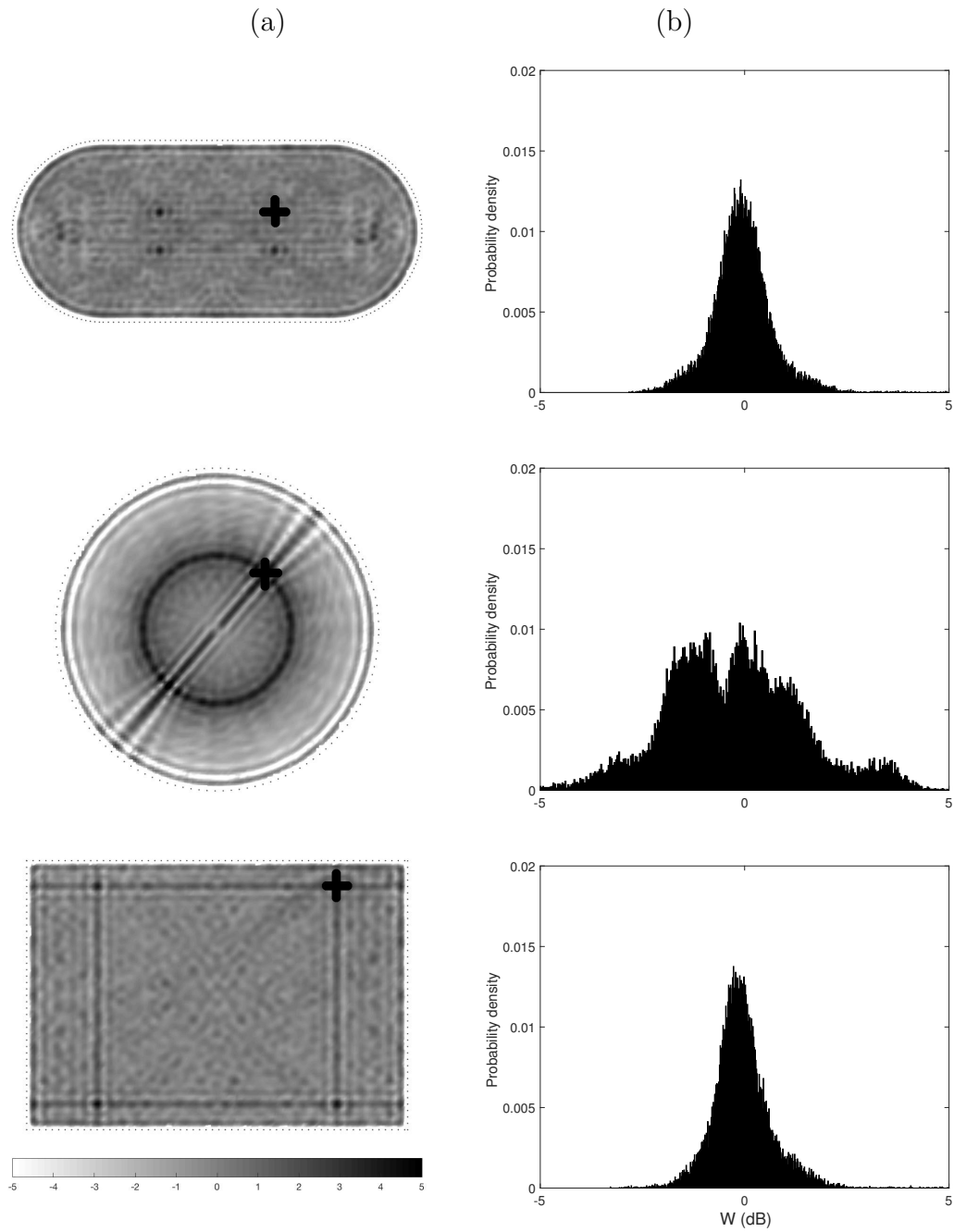


Figure 3: Flexural vibration of three different plates excited by a point force: top line, stadium; middle line, circle; bottom line, rectangle. (a) Distribution of energy density level (dB, ref=mean value). The dotted line in each figure represents the geometry boundary of plate. The cross indicates the force position. (b) Probability density function of energy density level.

ergy near the excitation point. This phenomena is caused by the near field which reaches a high value near the excitation point and quickly decreases with distance. Furthermore, the mean vibrational energy equals to zero at boundaries due to the boundary conditions.

4. Energy exchange between ergodic or non ergodic subsystems

Let us now examine the validity of the coupling power proportionality (2).

4.1. Presentation of the different cases

The most important condition for validity of statistical energy analysis is that the vibrational field is diffuse in all subsystems. There are mainly three ways to satisfy the condition of diffuse field in a subsystem. The first one is when the subsystem has a geometry which defines an ergodic billiard like the Bunimovich stadium. This guarantees that the vibrational field will be both homogeneous and isotropic. In this situation the nature of excitation is less important for emergence of diffusiveness. The second situation corresponds to a subsystem whose ray dynamics of underlying billiard imposes homogeneity or isotropy of vibrational field but not both at same time like the example of rectangle discussed in Section 3. In this case a further property of excitation is required to satisfy the counterpart condition in order to get diffusiveness. In the third situation, the subsystem has a geometry whose associated billiard is again non ergodic but whose ray dynamics does not impose neither homogeneity nor isotropy like the example of circular billiard. In this case, the excitation must enforce both homogeneity and isotropy in order to create diffusiveness. This will be reached with a rain-on-the-roof force field. In order to combine all possible ways to reach diffusiveness in numerical examples, let us consider the three types of plates shown in Table 2 and the three types of excitation shown in Table 3. The three considered excitations are respectively a rain-on-the-roof force field (uniform distribution of uncorrelated point forces), a point force (localized excitation with a uniform directivity), and a point torque (localized excitation with a non uniform directivity).

Five simulations are carried out to check whether the coupling power proportionality (2) is verified in these cases. In each simulation, two plates of same type P1, P2 or P3 and referenced by the subscript $i = 1, 2$ are coupled by a spring. The attachment point of spring is fixed to the centre on plate 2. Several different attachment points of spring on plate 1 are chosen for the

Plate	Geometry	Homogeneity	Isotropy
P1	Stadium	Yes	Yes
P2	Rectangle	Yes	No
P3	Circle	No	No

Table 2: Properties of three types of plates

Excitation	Type	Homogeneity	Isotropy
E1	Rain-on-the-roof	Yes	Yes
E2	Point force	No	Yes
E3	Point torque	No	No

Table 3: Properties of three types of excitations

calculation. The coordinates of these attachment points on plate 1 are given in Table 4. The excitation is applied on plate 1 with type chosen among E1, E2 and E3. The vibrational energies in each simulation are estimated by choosing 50 receivers at random on each plate.

The parameters for the simulation are the following. The plates are all made of steel with $E_0 = 210$ GPa, $\rho = 7800$ kg m⁻³, $\nu = 0.3$, and $\eta = 0.001$. The spring stiffness is $K = 1 \times 10^5$ N m⁻¹. The frequency band is an octave centred on $\omega_c = 2\pi \times 4000$ rad s⁻¹. All surface geometries are the same as in Section 3. The only change to be noticed is that in each simulation, plate 1 has thickness 2 mm and plate 2 has thickness 2.5 mm. For plate 1, the number of wavelengths, number of resonant modes, attenuation per mean-free-path and modal overlap have same values as in Table 1. For plate 2, these indicators are shown in Table 5.

The weak coupling condition is checked by values of connection strength $\kappa = K/(m_1 A_1 m_2 A_2 \omega^4)^{1/2}$, coupling strength $\gamma = 2\beta_{12}/(\pi M_1 M_2)$, and Smith's ratio $\sigma = \beta_{12}(1/M_1 + 1/M_2)$, where the modal overlap $M_i = \eta_i \omega n_i$ is estimated by Eq. (1) and β_{12} by Eq. (3). Their values are given in Table 6. Their small values show that all these systems of coupled plates are in the weak coupling regime (see [35] for comparison with other simulations from weak to strong coupling).

Case	point 1 (m)	point 2 (m)	point 3 (m)
A	(-0.3897, 0.2559)	(-0.3912, 0.1973)	(-0.3922, 0.1408)
B	(0.0046, 0.0033)	(0.0456, 0.0332)	(0.0913, 0.0663)
C	(0.0017, 0.0054)	(0.0174, 0.0537)	(0.0349, 0.1073)
D	(0.0046, 0.0033)	(0.0456, 0.0332)	(0.0913, 0.0663)
E	(0.0080, 0.3000)	(0.1200, 0.3000)	(0.2400, 0.3000)
Case	point 4 (m)	point 5 (m)	point 6 (m)
A	(-0.3943, 0.0194)	(-0.4000, -0.2187)	(-0.3993, -0.1730)
B	(0.1369, 0.0995)	(0.1826, 0.1326)	(0.2282, 0.1658)
C	(0.0523, 0.1610)	(0.0697, 0.2146)	(0.0872, 0.2683)
D	(0.1369, 0.0995)	(0.1826, 0.1326)	(0.2282, 0.1658)
E	(0.3600, 0.3000)	(0.4800, 0.3000)	(0.6400, 0.3000)
Case	point 7 (m)	point 8 (m)	point 9 (m)
A	(-0.2143, -0.1811)	(-0.0747, -0.1784)	(-0.0735, -0.0736)
B	(0.2739, 0.1990)	(0.3195, 0.2321)	(0.3652, 0.2653)
C	(0.1046, 0.3219)	(0.1220, 0.3756)	(0.1395, 0.4293)
D	(0.2739, 0.1990)	(0.3195, 0.2321)	(0.3652, 0.2653)
E	(0.8000, 0.3000)	(0.9200, 0.3000)	(1.0400, 0.3000)
Case	point 10 (m)	point 11 (m)	
A	(-0.3049, -0.1986)	(-0.3564, -0.2220)	
B	(0.4108, 0.2985)	-	
C	(0.1569, 0.4829)	-	
D	(0.4108, 0.2985)	-	
E	(1.1600, 0.3000)	-	

Table 4: Attachment points of spring on plate 1 in frames of Figs. 4-8

Plate 2	# Wavelength	# Modes	Attenuation	Modal overlap
Stadium	10.1	360	0.032	0.51
Circular	11.3	360	0.035	0.51
Rectangular	10.0	352	0.031	0.51

Table 5: Number of wavelength \bar{l}/λ , number of resonant modes N , attenuation per mean free path \bar{m} and modal overlap M of plate 2 at 4 kHz

Plates 1 and 2	Connection strength	Coupling strength	Smith's ratio
Stadium	9.1e-6	8.2e-5	1.5e-4
Circular	9.1e-6	8.2e-5	1.5e-4
Rectangular	9.1e-6	8.2e-5	1.5e-4

Table 6: Strength of coupling and connection. Connection strength κ , coupling strength γ , Smith's ratio σ

4.2. Numerical simulation

The numerical simulations aim to check for which systems the coupling power proportionality given in Eq. (2) applies. The factor β_{ij} is estimated by two calculations. In statistical energy analysis calculation, the factor is directly estimated by Eq. (3) and its value is noted $\beta_{12,SEA}$. The reference calculation is provided by a direct numerical simulation based on the following equations. The receptances of coupled systems are finely calculated for all frequencies in the band $[\omega_{\min}, \omega_{\max}]$ by the technique presented in Appendix. The factor is then estimated by

$$\beta_{12,REF} = \frac{P_{ij}}{\left(\frac{E_i}{n_i} - \frac{E_j}{n_j}\right)} \quad (7)$$

where the modal densities are given by (1).

For a point excitation, the mean vibrational energy in plate i is

$$E_i = \frac{S}{\pi} \iiint_{\omega_{\min}}^{\omega_{\max}} m_i \omega^2 |H_{i1}(x, y, x_0, y_0; \omega)|^2 d\omega dy dx \quad (8)$$

where $H_{i1}(x, y, x_0, y_0; \omega)$ denotes the receptance of coupled plates with a harmonic source located at x_0, y_0 in plate 1 and a receiver at x, y in plate i .

The mean power flowing from subsystem i to subsystem j is $P_{ij} = K \langle u_i \dot{u}_j \rangle$ where u_i, u_j are the plate deflections at the attachment point. Since the power spectral density S is confined in $[\omega_{\min}, \omega_{\max}]$, the exchanged power is obtained as

$$P_{ij} = K \frac{S}{\pi} \int_{\omega_{\min}}^{\omega_{\max}} \text{Re} [j\omega \bar{H}_{i1}(\chi, \xi, x_0, y_0; \omega) H_{j1}(\chi, \xi, x_0, y_0; \omega)] d\omega \quad (9)$$

where χ, ξ are the coordinates of the attachment point, the overbar denotes the complex conjugate, Re the real part, and j the imaginary unit. Details to calculate the receptance of coupled plates are given in Appendix.

These expressions of mean vibrational energy and the exchanged power can be generalised to a rain-on-roof excitation. A rain-on-roof excitation is defined as a random force field δ -correlated in space and time. It may be approximated by a large number of point forces randomly distributed in space and uncorrelated to each other. Let the excitation be in the general form of $f(x, y, t) = \sum_l F_l(t)\delta(x - x_l)\delta(y - y_l)$ where $F_l(t)$ is a random force with a power spectral density S constant in the frequency band $[\omega_{\min}, \omega_{\max}]$ and x_l, y_l the source position. As the forces are uncorrelated, one has $\langle F_k F_l \rangle = 0$ for $k \neq l$ that is the cross-power spectra are null. In this situation, the mean vibrational energy is

$$E_i = \frac{S}{\pi} \sum_l \iiint_{\omega_{\min}}^{\omega_{\max}} m_i \omega^2 |H_{i1}(x, y, x_l, y_l; \omega)|^2 d\omega dy dx \quad (10)$$

The exchanged power is

$$P_{ij} = K \frac{S}{\pi} \sum_l \int_{\omega_{\min}}^{\omega_{\max}} \text{Re} [j\omega \bar{H}_{i1}(\chi, \xi, x_l, y_l; \omega) H_{j1}(\chi, \xi, x_l, y_l; \omega)] d\omega \quad (11)$$

The point torque may be represented by two opposite forces separated by a small distance. In this situation, the mean vibrational energy is

$$E_i = \frac{S}{\pi} \iiint_{\omega_{\min}}^{\omega_{\max}} m_i \omega^2 |\Delta H_{i1}(x, y, x_0, y_0; \omega)|^2 d\omega dy dx \quad (12)$$

where $\Delta H_{i1}(x, y, x_0, y_0; \omega) = H_{i1}(x, y, x_1, y_1; \omega) - H_{i1}(x, y, x_2, y_2; \omega)$ and x_1, y_1 and x_2, y_2 are the positions of the two forces and x_0, y_0 their centre. The exchanged power is

$$P_{ij} = K \frac{S}{\pi} \int_{\omega_{\min}}^{\omega_{\max}} \text{Re} [j\omega \overline{\Delta H}_{i1}(\chi, \xi, x_0, y_0; \omega) \Delta H_{j1}(\chi, \xi, x_0, y_0; \omega)] d\omega \quad (13)$$

4.3. Analysis of the results

Let us now analyse the results for these cases.

(A) Stadium plates excited by a point torque . In this case, homogeneity and isotropy of vibrational field are guaranteed by ergodicity of stadium billiard , while a torque excitation provides neither homogeneity nor isotropy. The point torque is simulated by two out-of-phase forces respectively positioned at $x_0 = 0.1643$ m, $y_0 = 0.1767$ m and $x_0 = 0.1668$ m, $y_0 = 0.1810$ m on plate 1. The result is shown in Fig. 4. Satisfying the diffusiveness condition in each subsystem, $\beta_{1,2,SEA}$ is found to be in fine agreement with $\beta_{1,2,REF}$.

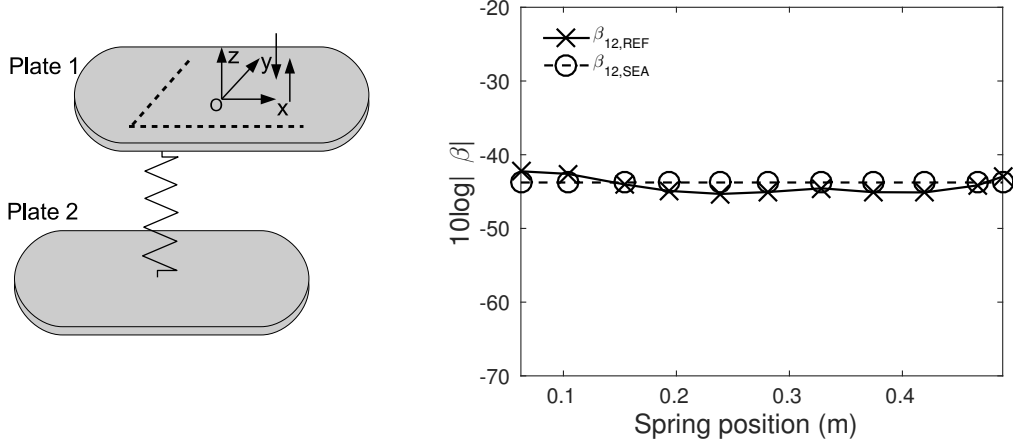


Figure 4: Comparison of energy transfer predicted by statistical energy analysis and reference calculation for two coupled stadium plates excited by a torque on plate 1. Factor β given by Eq. (3) and (7) versus position of coupling spring (dashed line in left).

(B) Circular plates excited by a point torque. In this case, there is no homogeneity nor isotropy from ray dynamics and there is no homogeneity or isotropy from excitation. This is typical example where the energy field on plate is much unevenly distributed violating the diffuse field assumption. The positions of the couple of forces simulating the torque are $x_0 = -0.4514$ m, $y_0 = 0$ m and $x_0 = -0.4513$ m, $y_0 = -0.0028$ m on plate 1. The result is shown in Fig. 5. A huge discrepancy between $\beta_{12,SEA}$ and $\beta_{12,REF}$ is shown.

(C) Circular plates excited by a point force. In this case, isotropy of vibrational field is guaranteed by point force excitation. However, neither structure nor excitation implies homogeneity. Diffuse field is not established in each plate. Fig. 6 shows the result for the point force position $x_0 = 0.16926$ m, $y_0 = 0$ m on plate 1. It is observed that there is a significant discrepancy between statistical energy analysis and reference calculation but less than the previous case.

(D) Circular plates excited by a rain-on-roof force field. In this case, homogeneity and isotropy of vibrational field are guaranteed by homogeneity and isotropy of rain-on-roof excitation, while the circular plate has neither of the two properties. To simulate the rain-on-roof excitation, 100 force positions are chosen at random on plate 1. The result in Fig. 7

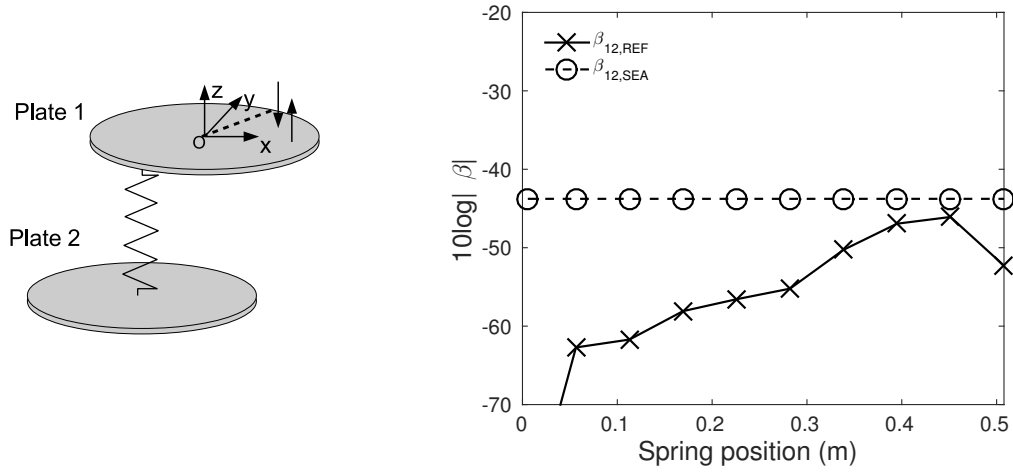


Figure 5: Comparison of energy transfer predicted by statistical energy analysis and reference calculation for two coupled circular plates excited by a torque on plate 1. Factors $\beta_{12,SEA}$ and $\beta_{12,REF}$ given by Eqs. (3) and (7) versus position of coupling spring (dashed line in left).

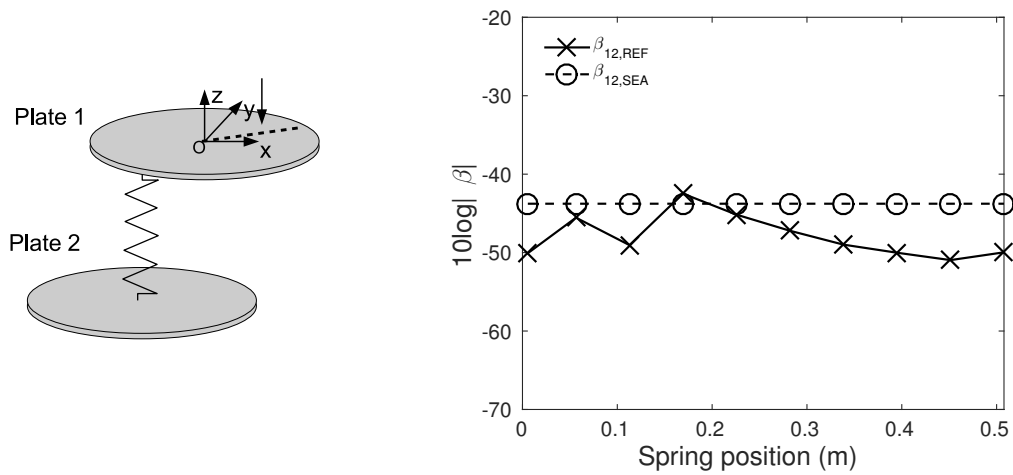


Figure 6: Comparison of energy transfer predicted by statistical energy analysis and reference calculation for two coupled circular plates excited by a point force on plate 1. Factors $\beta_{12,SEA}$ and $\beta_{12,REF}$ given by Eq. (3) and (7) versus position of coupling spring (dashed line in left).

shows that the prediction of statistical energy analysis and reference calculation are moderately in agreement. The reason for a moderate agreement is that despite plate 1 is applied with rain-on-roof excitation, the excitation on plate 2 caused by spring is always equivalent to a point force. Therefore the diffusiveness condition is not totally guaranteed on plate 2.

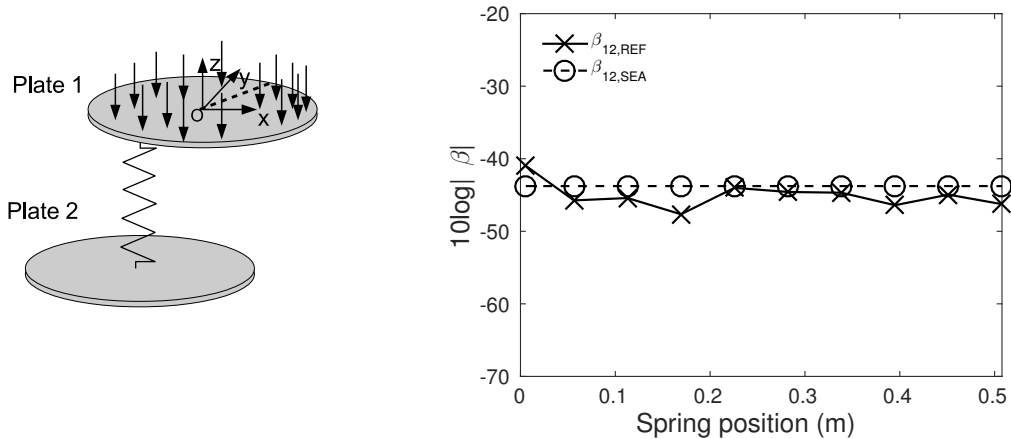


Figure 7: Comparison of energy transfer predicted by statistical energy analysis and reference calculation for two coupled circular plates excited by a rain-on-the-roof force on plate 1. Factors $\beta_{12,SEA}$ and $\beta_{12,REF}$ given by Eqs. (3) and (7) versus position of coupling spring (dashed line in left).

(E) Rectangular plates excited by a point force. In this case, homogeneity and isotropy of vibrational field are guaranteed by homogeneity of rectangular plate and isotropy of point force excitation. The result is shown in Fig. 8 for the point force position $x_0 = 0.8$ m, $y_0 = 0.56$ m on plate 1. It is observed that the prediction of statistical energy analysis and reference calculation are again in fine agreement.

5. Conclusion

In this paper, we have highlighted that in statistical energy analysis, the coupling power proportionality is valid if and only if a diffuse field is established in all subsystems. In particular, we have shown that the conditions of reverberation that is low damping and high number of resonant modes

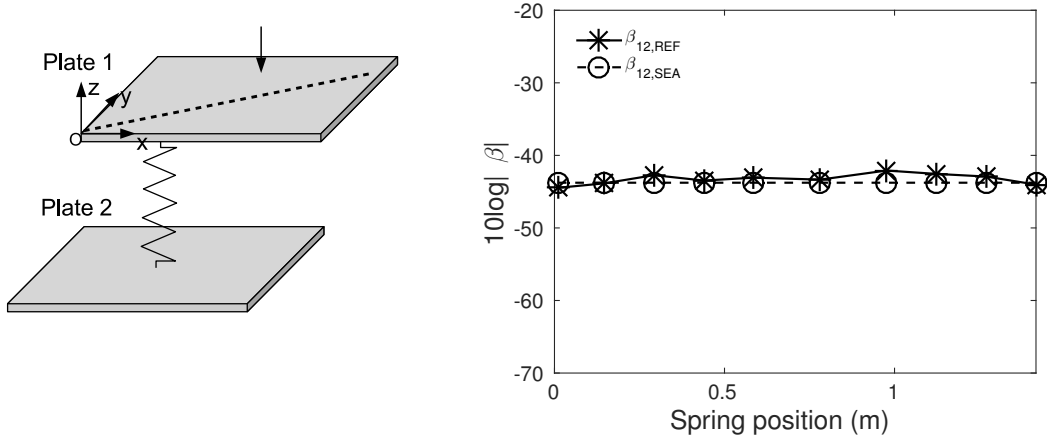


Figure 8: Comparison of energy transfer predicted by statistical energy analysis and reference calculation for two coupled rectangular plates excited by a point force on plate 1. Factors $\beta_{12,SEA}$ and $\beta_{12,REF}$ given by Eq. (3) and (7) versus position of coupling spring (dashed line in left).

are generally not enough to ensure the validity of statistical energy analysis. The other assumptions, weak and conservative couplings and wide-band, uncorrelated random sources, have not been discussed in this text but their importance has been underlined by many authors.

Diffusiveness of sound and vibration, that is homogeneity and isotropy of vibrational field, may result from two different causes. The geometrical properties of the domain may impose either homogeneity, isotropy, or both in case of ergodic billiards. This means that even if the source is a point excitation with strong directivity (like the torque considered in the examples), the resulting vibrational field will be diffuse in an ergodic billiard and therefore statistical energy analysis will apply successfully. The stadium plate presented in this paper is a good example. But the nature of sources plays a dual role and may also impose homogeneity when many point sources of same power cover the domain, or isotropy when directivity of sources is uniform. Diffusiveness of vibration and therefore applicability of statistical energy analysis may be obtained with rain-on-the-roof excitations even for non ergodic billiards as it has been observed on the circular plate.

Acknowledgements

The authors would like to thank Professor G. Tanner for the fruitful discussions we had on ray dynamics in billiards and for his valuable suggestions during the preparation of the manuscript.

This work was supported by the CNRS and Labex CeLyA of Université de Lyon, operated by the French National Research Agency (ANR-10-LABX-0060/ANR-11-IDEX-0007). This support is greatly appreciated.

6. Appendix

This appendix presents the calculation of receptance $H(\mathbf{r}, \mathbf{s}; \omega)$ where $\mathbf{r} = (x, y)$ is the receiver position and $\mathbf{s} = (x_0, y_0)$ the source position. Details to obtain receptance of single plates of Section 3 and receptance of coupled plates of Section 4 are given respectively as follows.

Single plate. For a single plate, on which a harmonic force $F \exp(j\omega t)$ is applied at point \mathbf{s} , the equation of motion of plate is

$$-m\omega^2 v + j\omega c v + D\Delta^2 v = F\delta_{\mathbf{s}} \quad (14)$$

where v is the transverse displacement of the plate, m the mass per unit area, c the viscous damping coefficient and D the bending stiffness. Δ^2 denotes the bi-Laplacian operator and $\delta_{\mathbf{s}}$ the Dirac distribution centred on \mathbf{s} .

Let ψ_n be the n th free mode (no resonator, no damping) of the plate and ω_n the eigenfrequency. The modes are orthogonal and conventionally normalized by $\int \psi_n(\mathbf{r})\psi_m(\mathbf{r})\mathbf{d}\mathbf{r} = \delta_{nm}$ where δ_{nm} is the Kronecker symbol. Since dissipation in Eq. (14) is modelled by a viscous damping coefficient proportional to the mass density, the displacement field $v(\mathbf{r})$ of the damped plate may be developed in the series of the undamped modes

$$v(\mathbf{r}) = \sum_n A_n \psi_n(\mathbf{r}) \quad (15)$$

By substituting Eq. (15) into the equation of motion (14) and by using the orthogonality property of normalized modes, $v(\mathbf{r})$ could be expressed as

$$v(\mathbf{r}) = \sum_n \frac{F\psi_n(\mathbf{s})\psi_n(\mathbf{r})}{m(\omega_n^2 + j\Delta\omega - \omega^2)} \quad (16)$$

where $\Delta = c/m$ is the half-power bandwidth. If a damping loss factor η is preferred then $\Delta = \eta\omega_n$.

The receptance of the plate is $H(\mathbf{r}, \mathbf{s}; \omega) = v(\mathbf{r})$, where a unit force $F = 1$ has been substituted. Thus, the expression of the receptance is obtained as

$$H(\mathbf{r}, \mathbf{s}; \omega) = \sum_n \frac{\psi_n(\mathbf{s})\psi_n(\mathbf{r})}{m(\omega_n^2 + j\Delta\omega - \omega^2)} \quad (17)$$

Coupled plates. Let $H_{ij}(\mathbf{r}, \mathbf{s}; \omega)$ be the receptance of 2 plates coupled through springs of stiffness K . Each plate has its proper uncoupled receptance noted $H_i(\mathbf{r}, \mathbf{s}; \omega)$, which can be calculated by the previous method. Assuming that a harmonic point force $F\exp(j\omega t)$ is applied to plate j at point \mathbf{s} , the displacement in plate i at point \mathbf{r} is

$$v_i(\mathbf{r}) = F\delta_{ij}H_i(\mathbf{r}, \mathbf{s}; \omega) + \sum_k R_{ik}H_i(\mathbf{r}, \mathbf{r}_{ik}; \omega) \quad (18)$$

where R_{ik} represents the reaction applied by plate k onto plate i through the coupling spring at position \mathbf{r}_{ik} . The term δ_{ij} means that the point load is applied only on plate j .

The reaction R_{ik} is

$$R_{ik} = K[v_k(\mathbf{r}_{ki}) - v_i(\mathbf{r}_{ik})] \quad (19)$$

Then, by replacing Eq. (19) into Eq. (18) and taking $F = 1$, the receptance $H_{ij}(\mathbf{r}, \mathbf{s}; \omega)$ of the plate i in the coupled system is

$$H_{ij}(\mathbf{r}, \mathbf{s}; \omega) = \delta_{ij}H_i(\mathbf{r}, \mathbf{s}; \omega) + \sum_k K[v_k(\mathbf{r}_{ki}) - v_i(\mathbf{r}_{ik})]H_i(\mathbf{r}, \mathbf{r}_{ik}; \omega) \quad (20)$$

By substituting $\mathbf{r} = \mathbf{r}_{ik}$ into Eq. (20), one obtains a set of linear equations on the unknowns $v_i(\mathbf{r}_{ik})$. The set of linear equations is

$$v_i(\mathbf{r}_{ik}) = \delta_{ij}H_i(\mathbf{r}_{ik}, \mathbf{s}; \omega) + \sum_{k'} K[v_{k'}(\mathbf{r}_{k'i}) - v_i(\mathbf{r}_{ik'})]H_i(\mathbf{r}_{ik}, \mathbf{r}_{ik'}; \omega) \quad (21)$$

For the calculation of two coupled plates, a unique spring is attached at \mathbf{r}_{12} on plate 1 and \mathbf{r}_{21} on plate 2. The excited plate is $j = 1$. The two receptances $H_{i1}(\mathbf{r}, \mathbf{s}; \omega)$ form a column vector $\mathbf{H} = (H_{11}, H_{21})^T$ given by

$$\mathbf{H}(\mathbf{r}, \mathbf{s}; \omega) = K\Psi(\mathbf{r})\mathbf{V} + \mathbf{F}(\mathbf{r}) \quad (22)$$

where $\mathbf{V} = (v_1(\mathbf{r}_{12}), v_2(\mathbf{r}_{21}))^T$, $\mathbf{F}(\mathbf{r}) = (H_1(\mathbf{r}, \mathbf{s}; \omega), 0)^T$ and

$$\Psi(\mathbf{r}) = \begin{bmatrix} -H_1(\mathbf{r}, \mathbf{r}_{12}; \omega) & H_1(\mathbf{r}, \mathbf{r}_{12}; \omega) \\ H_2(\mathbf{r}, \mathbf{r}_{21}; \omega) & -H_2(\mathbf{r}, \mathbf{r}_{21}; \omega) \end{bmatrix} \quad (23)$$

The unknowns are determined by the system

$$(\mathbf{I} + K\Phi)\mathbf{V} = \mathbf{F}_0 \quad (24)$$

where \mathbf{I} is the 2×2 identity matrix and $\mathbf{F}_0 = (H_1(\mathbf{r}_{12}, \mathbf{s}; \omega), 0)^T$. The matrix Φ is

$$\Phi(\mathbf{r}) = \begin{bmatrix} H_1(\mathbf{r}_{12}, \mathbf{r}_{12}; \omega) & -H_1(\mathbf{r}_{12}, \mathbf{r}_{12}; \omega) \\ -H_2(\mathbf{r}_{21}, \mathbf{r}_{21}; \omega) & H_2(\mathbf{r}_{21}, \mathbf{r}_{21}; \omega) \end{bmatrix} \quad (25)$$

With the unknowns solved by Eq. (24), the receptances can be determined by Eq. (22) at all points \mathbf{r} for any excitation point \mathbf{s} .

References

- [1] A. Le Bot, *Foundation of statistical energy analysis in vibroacoustics*, Oxford University Press, Oxford, 2015.
- [2] R.H. Lyon, G. Maidanik, Power flow between linearly coupled oscillators, *J. Acoust. Soc. Am.* **34** (1962) 623-639.
- [3] P.W. Smith, Response and radiation of structural modes excited by sound. *J. Acoust. Soc. Am.*, **34** (1962) 640–647.
- [4] D.E. Newland, Calculation of power flow between coupled oscillators, *J. Sound Vib.* **3** (1966) 262-276.
- [5] D.E. Newland, Power flow between a class of coupled oscillators, *J. Acoust. Soc. Am.* **43** (1968) 553-559.
- [6] T.D. Scharton, R.H. Lyon, Power flow and energy sharing in random vibration, *J. Acoust. Soc. Am.* **43** (1968) 1332-1343.
- [7] E. Luzzato, E. Ortola, The characterization of energy flow paths in the study of dynamics systems using SEA theory, *J. Sound Vib.* **123** (1988) 189-197.
- [8] R.J.M. Craik, Sound transmission paths through a statistical energy analysis model, *Applied Acoustics* **30** (1990) 45-55.

- [9] O. Guasch, A. Aragonès, Finding the dominant energy transmission paths in statistical energy analysis, *J. SOund Vib.* **330** (2011) 2325-2338.
- [10] W.C. Sabine, *Collected papers on acoustics*, Harvard University Press, Cambridge, MA, 1922.
- [11] A. Le Bot, Entropy in Statistical Energy Analysis, *J. Acoust. Soc. Am.* **125** (2009) 1473-1478.
- [12] A. Le Bot, A. Carcaterra, D. Mazuyer, Statistical vibroacoustics and entropy concept, *Entropy* **12** (2010) 2418-2435.
- [13] D.A. Tufano, Z. Sotoudeh, Entropy in strongly coupled oscillators, *J. Vib. Acoust.* **140** (2017) 011003.
- [14] A. Le Bot, Entropy in sound and vibration: towards a new paradigm, *Proc. R. Soc. A* **473** (2017) 20160602.
- [15] F.J. Fahy, Statistical energy analysis: A critical overview. In *Statistical energy analysis an overview with applications in structural dynamics* Edited by A.J. Keane and W.G. Price, Cambridge University Press, Cambridge, 1994.
- [16] C.B. Burroughs, R.W. Fisher, F.R. Kern, An introduction to statistical energy analysis, *J. Acoust. Soc. Am.*, **101**, (1997) 1779–1789.
- [17] B.R. Mace, L. Ji, The statistical energy analysis of coupled sets of oscillators, *Proceedings of the royal society A* **463** (2007) 1359-1377.
- [18] T. Lafont, N. Totaro, A. Le Bot, Review of statistical energy analysis hypotheses in vibroacoustics, *Proc. R. Soc. A* **470** (2013) 20130515.
- [19] J.L. Guyader, N. Totaro, L. Maxit, Statistical Energy Analysis with fuzzy parameters to handle populations of structures, *J. Sound Vib.* **379** (2016) 119-134.
- [20] W. Joyce, Sabine’s reverberation time and ergodic auditoriums, *J. Acoust. Soc. Am.* **58** (1975) 643-655.

- [21] J.D. Polack, Playing billiards in the concert hall: the mathematical foundations of geometrical room acoustics, *Applied Acoustics* **38** (1993) 235-244.
- [22] G. Tanner, N. Søndergaard, Waves chaos in acoustics and elasticity, *J. Phys. A* **40** (2007) 443-509.
- [23] D.J. Chappell, D. Löchel, N. Søndergaard, G. Tanner, Dynamical energy analysis on mesh grids: A new tool for describing the vibro-acoustic response of complex mechanical structures, *Wave Motion* **51** (2014) 589-597.
- [24] A. Le Bot, E. Sadoulet-Reboul, High frequency vibroacoustics: A radiative transfer equation and radiosity based approach, *Wave Motion* **51** (2014) 598-605.
- [25] A. Le Bot, Derivation of statistical energy analysis from radiative exchanges, *J. Sound Vib.* **300** (2007) 763-779.
- [26] A. Le Bot, V. Cotoni, Validity diagrams of statistical energy analysis, *J. Sound Vib.* **329** (2010) 221-235.
- [27] B.R. Mace, The statistical energy analysis of two continuous one-dimensional subsystems, *J. Sound Vib.* **166** (1993) 429-461.
- [28] S. Finnveden, Ensemble averaged vibration energy flows in a three element structure, *J. Sound Vib.* **187** (1995) 495-529.
- [29] S. Finnveden, A quantitative criterion validating coupling power proportionality in statistical energy analysis, *J. Sound Vib.*, **330** (2011) 87-109.
- [30] P.W. Smith, Statistical models of coupled dynamical systems and the transition from weak to strong coupling, *J. Acoust. Soc. Am.* **65** (1979) 695-698.
- [31] G. Tanner, Dynamical energy analysis - Determining ave energy distributions in vibro-acoustical structures in the high-frequency regime, *J. Sound Vib.* **320** (2009) 1023-1038.
- [32] R.L. Weaver, On diffuse waves in solid media, *J. Acoust. Soc. Am.* **71** (1982) 1608-1609.

- [33] H.J. Korsch, F. Zimmer, Chaotic billiards, In Computational statistical physics, Springer, Berlin, 2002.
- [34] M.V. Berry, Regularity and chaos in classical mechanics, illustrated by three deformations of a circular 'billiard', Eur. J. Phys. **2** (1981) 91-102.
- [35] T. Lafont, N. Totaro, A. Le Bot, Coupling strength assumption in statistical energy analysis, Proc. R. Soc. A **473** (2017) 20160927.